

1 Spatio-temporal patterns of the effects of precipitation variability
2 and land use/cover changes on long-term changes in sediment yield
3 in the Loess Plateau, China

4
5 Revised manuscript submitted to *Hydrology and Earth System Sciences* (hess-2016-654)

6
7 Guangyao Gao^{1,2}, Jianjun Zhang¹, Yu Liu³, Zheng Ning¹, Bojie Fu^{1,2}, and Murugesu
8 Sivapalan^{4,5}

9
10 ¹State Key Laboratory of Urban and Regional Ecology, Research Center for
11 Eco-Environmental Sciences, Chinese Academy of Sciences, Beijing 100085, China

12 ²Joint Center for Global Change Studies, Beijing 100875, China

13 ³Key Laboratory of Ecosystem Network Observation and Modeling, Institute of Geographical
14 Sciences and Natural Resources Research, Chinese Academy of Sciences, Beijing 100101,
15 China

16 ⁴Department of Geography and Geographic Information Science, University of Illinois at
17 Urbana-Champaign, Champaign, Illinois, USA

18 ⁵Department of Civil and Environmental Engineering, University of Illinois at
19 Urbana-Champaign, Urbana, Illinois, USA

20
21 *Correspondence to:* Guangyao Gao (gygao@rcees.ac.cn)

22
23 **Abstract**

24 Within China's Loess Plateau there have been concerted revegetation efforts and
25 engineering measures since the 1950s aimed at reducing soil erosion and land degradation.

26 As a result, annual streamflow, sediment yield and sediment concentration have all
27 decreased considerably. Human induced land use/cover change (LUCC) was the dominant
28 factor, contributing over 70% of the sediment load reduction, whereas the contribution of
29 precipitation was less than 30%. In this study, we use 50-year time series data (1961-2011),
30 showing decreasing trends in the annual sediment loads of fifteen catchments, to generate
31 spatio-temporal patterns in the effects of LUCC and precipitation variability on sediment
32 yield. The space-time variability of sediment yield was expressed notionally as a product of
33 two factors representing: (i) effect of precipitation and (ii) fraction of treated land surface
34 area. Under minimal LUCC, the square root of annual sediment yield varied linearly with
35 precipitation, with the precipitation-sediment load relationship showing coherent spatial
36 patterns amongst the catchments. As the LUCC increased and took effect, the changes of
37 sediment yield pattern depended more on engineering measures and vegetation restoration
38 campaign, and the within-year rainfall patterns (especially storm events) also played an
39 important role. The effect of LUCC is expressed in terms of a sediment coefficient, i.e.,
40 ratio of annual sediment yield to annual precipitation. Sediment coefficients showed a
41 steady decrease over the study period, following a linear decreasing function of the fraction
42 of treated land surface area. In this way, the study has brought out the separate roles of
43 precipitation variability and LUCC in controlling spatio-temporal patterns of sediment
44 yield at catchment scale.

45
46 **Keywords:** Loess Plateau, sediment yield, land use/land cover change, climate change,
47 precipitation variability

48 **1 Introduction**

49 Streamflow and sediment transport are important controls on biogeochemical processes
50 that govern ecosystem health in river basins (Syvitski, 2003). Changes in soil erosion on
51 landscapes and the resulting changes in sediment transport rates in rivers have great
52 environmental and societal consequences, particularly since they can be brought about by
53 climatic changes and human induced land use/cover changes (LUCC) (Syvitski, 2003;
54 Beechie et al., 2010). Understanding the dominant mechanisms behind such changes at
55 different time and space scales is crucial to the development of strategies for sustainable
56 land and water management in river basins (Wang et al., 2016).

57 In recent decades, streamflows and sediment yields in large rivers throughout the world
58 have undergone substantial changes (Milly et al., 2005; Nilsson et al., 2005; Milliman et al.,
59 2008; Cohen et al., 2014). Notable decreases in sediment yields have been observed in
60 approximately 50% of the world's rivers (Walling and Fang, 2003; Syvitski et al., 2005).
61 Many studies have investigated the dynamics of streamflows and sediment yields at
62 different spatial and temporal scales (Mutema et al., 2015; Song et al., 2016; Gao et al.,
63 2016; Tian et al., 2016). In addition to climate variability, LUCC, soil and water
64 conservation measure (SWCM) and construction of reservoirs and dams have substantially
65 contributed to the sediment load reductions (Walling, 2006; Milliman et al., 2008; Wang et
66 al., 2011). While previous studies have certainly provided valuable insights into the
67 streamflow and sediment load changes, the distinctive roles of LUCC and precipitation
68 variability in changing sediment loads still need further investigation in large domains and
69 across gradients of climate and land surface conditions (Walling, 2006; Mutema et al.,

70 2015). A particularly useful approach to the development of generalizable understanding of
71 the effects of precipitation variability and LUCC is a comparative analysis approach
72 focused on extracting spatio-temporal patterns of sediment yields based on observations in
73 multiple locations within the same region, or even across different regions. This is
74 especially valuable and crucial in areas with severe soil erosion and fragile ecosystems, e.g.,
75 the Loess Plateau (LP) in China, which is the motivation for the work presented in this
76 paper.

77 The LP lies in the middle reaches of the Yellow River (YR) Basin, and contributes
78 nearly 90% of the YR sediment (Wang et al., 2016). The historically severe soil erosion in
79 the LP is due to sparse vegetation, intensive rainstorms, erodible loessial soil, steep
80 topography and a long agricultural history (Rustomji et al., 2008). To control such severe
81 soil erosion, several SWCMs, including terrace and check-dam construction, afforestation
82 and pasture reestablishment, have been implemented since the 1950s (Yao et al., 2011;
83 Zhao et al., 2017). A large ecological restoration campaign, the Grain-for-Green (GFG)
84 project converting farmland on slopes exceed 25° to forest and pasture lands, was launched
85 in 1999 (Chen et al., 2015). Furthermore, the climate in the LP region has been showing
86 both warming and drying trends (i.e. increased potential evapotranspiration and reduced
87 precipitation) since the 1950s (Zhang et al., 2016).

88 These substantial LUCC have notably altered the hydrological regimes of the LP in
89 combination with the climate change. Consequently, the sediment yields within the LP have
90 showed a predictable declining trend over the past 60 years (Zhao et al., 2017), resulting in
91 approximately a 90% decrease of sediment yield in the YR (Miao et al., 2010, 2011; Wang

92 et al., 2016). Many other studies have detected the influences of LUCC and precipitation
93 variability on sediment load changes within the LP. Rustomji et al. (2008) estimated that
94 the contribution of catchment management practices to the decrease of annual sediment
95 yield ranged between 64 and 89% for eleven catchments in the LP during 1950s-2000.
96 Zhao et al. (2017) examined the spatio-temporal variation of sediment yield from 1957 to
97 2012 across the LP, and indicated that the adoption of large-scale SWCMs led to significant
98 reduction of sediment yield between Toudaoguai and Tongguan stations and large
99 reservoirs operation played a critical role in sediment yield reduction between Tongguan
100 and Huayuankou stations. Zhang et al. (2016) pointed that the combined effects of climate
101 aridity, engineering projects and vegetation cover change have induced significant
102 reductions of sediment yield between 1950 and 2008. Wang et al. (2016) found that
103 engineering measures for soil and water conservation were the main factors for the
104 sediment load decrease between the 1970s and 1990s, but large-scale vegetation restoration
105 campaigns also played an important role in reducing soil erosion since the 1990s.

106 On the basis of the outcomes of these studies, it is now generally accepted that the
107 largest reductions of sediment yield within the LP resulted from LUCC. However, this is
108 general knowledge covering the whole region, and given the significant variability of
109 climate and catchment characteristics across the LP (Sun et al., 2015a; Sun et al., 2015b), it
110 is important to go further and explore how these might affect spatio-temporal patterns of
111 sediment yield. Exploration of these patterns is important for sustainable ecosystem
112 restoration and water resources planning and management within the LP. They will also
113 serve as the basis for future research aimed at the development of more generalizable

114 understanding of landscape and climate controls on sediment yields at the catchment scale.

115 Most of the sediment yield of the LP was produced in the Coarse Sandy Hilly
116 Catchments (CSHC) region (Fig. 1) located in the central region of the LP. The CSHC
117 supplied over 70% of total sediment load in the YR, especially coarse sand (Rustomji et al.,
118 2008). This region was the focus of our efforts to investigate the variation of sediment load
119 from 15 catchments within the region within the LP. The specific objectives of this study
120 were, therefore, to: (1) attribute the temporal changes in sediment yield to changes in both
121 precipitation variability and LUCC over the entire study period (1961-2011) within the
122 CSHC region, (2) extract spatio-temporal trends in sediment yields on the basis of annual
123 sediment yield data, (3) separate the contributions of precipitation variability and fractional
124 area of LUCC to the observed spatio-temporal patterns of sediment yields, and pave the
125 way for more detailed process-based studies in the future.

126 **2 Materials and methods**

127 **2.1 Study area**

128 The CSHC region covers the area between the Toudaoguai and Longmen hydrological
129 stations in the mainstream of the YR (Fig. 1). The main stream that flows through the
130 CSHC region is 733 km long and its drainage catchment covers $12.97 \times 10^4 \text{ km}^2$, which is
131 accounting for 14.8% of the entire YR Basin. The CSHC region is characterized by arid to
132 semi-arid climate conditions. The annual precipitation in the region during 1961-2011 was
133 437 mm on average, and varied from lower than 300 mm in the northwest to 580 mm in the
134 southeast (McVicar et al., 2007). The precipitation that occurs during the flood season
135 (June-September) is usually in the form of rainstorms with high intensity and accounts for

136 72% of the annual rainfall total. Correspondingly, about 45% of the annual runoff and 88%
137 of the annual sediment yield within the region are produced during the flood season. The
138 northwestern part of the CSHC is relatively flat while the southeastern part is more finely
139 dissected (Rustomji et al., 2008).

140 Fourteen main catchments along a north-south transect within the CSHC study area
141 were chosen for the study (Fig. 1). These catchments account for 57.4% of the CSHC area,
142 and contribute about 70% and 72% of streamflow and sediment load of the overall CSHC,
143 respectively, based on observed hydrological data during 1961-2011 (Rustomji et al., 2008;
144 Yao et al., 2011). Characteristics of these catchments are presented in Table 1 and Fig. 2,
145 showing that the catchments present strong climate and land surface gradients. The
146 catchments in the northwestern part (#1-6) had relatively lower mean annual precipitation
147 ($380 \text{ mm} < \bar{P} < 445 \text{ mm}$, where \bar{P} is mean annual precipitation over 1961-2011) and low
148 growing season (April-October) LAI ($0.41 < \text{LAI} < 0.48$, where LAI is the leaf area index),
149 while the corresponding values for catchments in the southeastern part (#7-14) were
150 470-570 mm and $0.63 < \text{LAI} < 3.26$, respectively.

151 The entire CSHC region is considered as an additional “catchment” and it is also
152 examined independently. The streamflow and sediment load for the whole region were
153 taken to be equal to the differences of corresponding measurements between the
154 Toudaoguai and Longmen gauging station. The average annual precipitation, streamflow
155 and sediment load of the region during 1961-2011 was 437.27 mm, 33.30 mm and 5.17 Gt,
156 respectively. Both the annual river discharge and sediment load across the region showed
157 significant decreasing trends (-0.82 mm yr^{-1} , $p < 0.001$ and -0.19 Gt yr^{-1} , $p < 0.001$,

158 respectively) over the past five decades, whereas precipitation decreased only slightly
159 (-0.93 mm yr^{-1} , $p=0.25$) (Fig. 3).

160 **2.2 Data collection**

161 Monthly streamflow and sediment load data during 1961-2011 were provided by the
162 Yellow River Conservancy Commission of China. Daily rainfall data from 1961 to 2011 at
163 66 meteorological stations in and around the region (Fig. 1) were obtained from the
164 National Meteorological Information Center of China. The spatially average of rainfall data
165 was carried out using the co-kriging interpolation algorithm with the DEM as an additional
166 input. The hydro-meteorological data (including annual precipitation, P [mm], streamflow,
167 Q [mm], and sediment load, S [t]), specific sediment yield defined as $SSY=S/A$ [t km^{-2}],
168 where A is the drainage area of the hydrological station [km^2], sediment concentration
169 defined as $SC=S/(Q.A)$ [kg m^{-3}] and the sediment coefficient defined as $C_s=SSY/P$ [t km^{-2}
170 mm^{-1}] were estimated for each catchment.

171 The mean catchment slope gradient based on the ASTER GDEM data with a resolution of
172 30 m and soil data (scale 1:500,000) were provided by the National Earth System Science
173 Data Sharing Infrastructure (<http://www.geodata.cn>). The land use information as at 1975,
174 1990, 2000 and 2010 was determined with Landsat MSS and TM remote sensing images at a
175 spatial resolution of 30 m. Six land use types were classified, i.e., forestland, cropland,
176 grassland, construction land, water body, and barren land. The LAI data during 1982-2011
177 were obtained from the Global Land Surface Satellite (GLASS) NDVI Series with spatial
178 resolution of 1 km (www.landcover.org, Zhao et al., 2013). The total areas impacted by
179 various SWCMs (i.e., afforestation, grass plantation, terraces and check-dams) in each

180 catchment during 1960s-2000s were obtained from Yao et al. (2011).

181 **2.3 Trend test**

182 The non-parametric Mann-Kendall (M-K) test method proposed by Mann (1945) and
183 Kendall (1975) was used to determine the significance of the trends in annual
184 meteorological and hydrological time series. A precondition for using the MK test is to
185 remove the serial correlation of climatic and hydrological series. In this study, the
186 trend-free pre-whitening (TFPW) method of Yue and Wang (2002) was used to remove the
187 auto-correlations before the trend test. There was no residual autocorrelation remaining
188 after performing the TFPW. A Z-statistic was obtained from the M-K test on the whitened
189 series. A negative value of Z indicates a decrease trend, and vice versa. The magnitude of
190 the slope of the trend (β) was estimated by (Sen, 1968; Hirsch et al., 1982):

$$191 \quad \beta = \text{Median} \left[\frac{x_j - x_i}{j - i} \right] \quad \text{for all } i < j \quad (1)$$

192 where x_i and x_j are the sequential data values in periods i and j , respectively.

193 **2.4 Attribution analysis of changes in sediment yield**

194 The time-trend analysis method was used to determine the quantitative contributions of
195 LUCC and precipitation variability to sediment yield changes. This method is primarily
196 designed to determine the differences in hydrological time series between different periods
197 (reference and validation periods) with different LUCC conditions (Zhang et al., 2011). In
198 this method, a regression equation between precipitation and sediment yield is developed
199 and evaluated during the reference period, and the established equation is then used to
200 estimate sediment yield during the validation period. The difference between measured and
201 predicted sediment yields during the validation period represents the effects of LUCC, and

202 the residual changes are caused by precipitation variability. The governing equations of the
 203 time-trend analysis method can be expressed as:

$$204 \quad SSY_1 = f(P_1) \quad (2)$$

$$205 \quad SSY'_2 = f(P_2) \quad (3)$$

$$206 \quad \Delta SSY^{LUCC} = \overline{SSY_2} - \overline{SSY'_2} \quad (4)$$

$$207 \quad \Delta SSY^{Pre} = (\overline{SSY_2} - \overline{SSY_1}) - \Delta SSY^{LUCC} \quad (5)$$

208 where SSY' is the predicted sediment yield, subscripts 1 and 2 indicate the reference and
 209 validation periods, respectively. $\overline{SSY_1}$ and $\overline{SSY_2}$ represent mean measured sediment yield
 210 during the reference and validation periods, respectively, and $\overline{SSY'_2}$ represents mean
 211 predicted sediment yield during the validation period. ΔSSY^{LUCC} and ΔSSY^{Pre} are sediment
 212 yield changes during the validation period associated with LUCC and precipitation
 213 variability, respectively. Rustomji et al. (2008) found that the square root of annual
 214 sediment yield in the catchments of the Loess Plateau was linearly related to annual
 215 precipitation. This was, therefore, used in this study as the motivation to develop the
 216 precipitation-sediment yield relationship during the reference period:

$$217 \quad \sqrt{SSY} = aP + b \quad (6)$$

218 In this study, the full data period of 1961-2011 was divided into three phases
 219 (1961-1969, 1970-1999 and 2000-2011). The first period was considered the reference
 220 period as the effects of human activities were slight and could be ignored (Wang et al.,
 221 2016). During the second stage, numerous SWCMs were implemented. For the third stage,
 222 a large ecological restoration campaign (GFG project) was launched in 1999.

223 **3 Results and discussion**

224 **3.1 Changes of land use/cover**

225 The CSHC region has undergone extensive LUCC caused by the implementation of
226 SWCM and vegetation restoration projects (e.g., the GFG project). Fig. 4 shows the
227 distribution of land use types of the region in 1975, 1990, 2000 and 2010. More than 90%
228 of the whole area was occupied by the cropland, forestland and grassland. The area of
229 cropland decreased by 26.72% and forestland increased by 53.15%, and there was no
230 significant change for the area of grassland (increase of 4.21%) in the CSHC region from
231 1975-2010. The majority of changes occurred during 2000-2010 due to the GFG
232 (reforestation) project (26.67% decrease and 36.21% increase for cropland and forestland,
233 respectively). The transition from cropland to forestland was greater in the catchments of
234 the southeastern part (especially in catchments #7-#9) than that in the northwestern part
235 (Fig. 4). In the period 1975 to 2000, the increase of forestland was 26.34% and 4.55% in
236 the southeastern and northwestern part, respectively, and the change of cropland was
237 negligible (only -0.39% and 0.22%, respectively). During 2000-2010, the forestland
238 increased by 47.79% and 18.30%, and the cropland decreased by 44.84% and 21.04% in
239 the southeastern and northwestern part, respectively.

240 The SWCMs implemented in the LP included both biotic treatments (e.g., afforestation
241 and grass-planting) and engineering measures (e.g., construction of terrace and check-dam
242 and gully control projects). Afforestation, grass-planting and construction of terraces were
243 seen as the slope measures, while building of check-dams and gully control projects were
244 the measures on the river channel. Although the area utilized for engineering measures was
245 much smaller than the biotic treatments, they immediately and substantially trap

246 streamflow and sediment load. The fraction of the treated area (area treated by erosion
247 control measures relative to total catchment area) increased from 3.95% in the 1960s to
248 28.61% in the 2000s (Fig. 5). The increase of the treated area was greatest during the 1980s
249 as a result of comprehensive management of small watersheds and the 2000s due to the
250 GFG project since 1999. Some decreases of SWCM areas (i.e. afforestation and
251 check-dams) occurred during the 1990s (Fig. 5) as some planted trees were died due to
252 drought and some small and medium check-dams were fully deposited by sediment and
253 then subsequently destroyed by floods.

254 The growing season LAI of the whole region changed from 0.74 during 1982-1999 to
255 0.81 during 2000-2011, an increase of 10.16% (Fig. 5). The LAI did not show significant
256 increase during 1982-1999 (0.003 yr^{-1} , $p=0.11$), and it increased significantly during
257 2000-2011 (0.024 yr^{-1} , $p<0.01$). The increase of growing season LAI during 1982-2011
258 was greater for the catchments in the southeastern part (0.009 yr^{-1}) compared to the
259 northwestern part (0.004 yr^{-1}), especially after 2000 (Fig. 6). In the period from 1982-1999
260 to 2000-2011, the average increase of growing LAI of the fourteen sub-catchments was
261 0.088 yr^{-1} ($0.010\text{-}0.183 \text{ yr}^{-1}$), with the increase of 0.114 yr^{-1} and 0.053 yr^{-1} in the
262 southeastern and northwestern part, respectively.

263 **3.2 Trends of hydro-meteorological and sediment yield variables**

264 Table 2 shows the trends in annual P , Q , SSY , SC and C_s of the fifteen catchments during the
265 period 1961-2011. The annual P showed a decline trend in all catchments except the Jialu
266 catchment, but the changing trend is only significant in the Xinshui and Zhouchuan
267 catchments ($p<0.05$). The annual Q , SSY , SC and C_s showed significant decreasing trends in

268 all the catchments, and most of the decreases were at the 0.001 significance level. For the
269 fourteen sub-catchments, the average decrease rates of annual values of Q , SSY , SC and C_s
270 were 0.86 mm yr^{-1} ($0.24\text{-}1.66 \text{ mm yr}^{-1}$), $190.06 \text{ t km}^{-2} \text{ yr}^{-1}$ ($26.47\text{-}398.82 \text{ t km}^{-2} \text{ yr}^{-1}$), 2.73
271 $\text{kg m}^{-3} \text{ yr}^{-1}$ ($0.69\text{-}4.70 \text{ kg m}^{-3} \text{ yr}^{-1}$) and $0.38 \text{ t km}^{-2} \text{ mm}^{-1} \text{ yr}^{-1}$ ($0.04\text{-}0.87 \text{ t km}^{-2} \text{ mm}^{-1} \text{ yr}^{-1}$),
272 respectively. The changing rates of Q , SSY , SC and C_s for the whole region were -0.85 mm
273 yr^{-1} , $-131.52 \text{ t km}^{-2} \text{ yr}^{-1}$, $-2.06 \text{ kg m}^{-3} \text{ yr}^{-1}$ and $-0.27 \text{ t km}^{-2} \text{ mm}^{-1} \text{ yr}^{-1}$, respectively. The annual
274 average reductions in the whole region were equivalent to 2.56%, 3.30%, 2.01% and 3.07%
275 of the mean annual values of Q , SSY , SC and C_s , respectively.

276 The mean and the coefficient of variation, C_v , representing inter-annual variability of
277 annual values of P , Q , SSY , SC and C_s for the fifteen catchments during the three phases
278 (reference period-1, period-2 and period-3) are shown in Fig. 7. Compared to standard
279 deviation, the C_v value was better able to indicate the inter-annual variability of precipitation,
280 streamflow and sediment load among the catchments with distinctly different average values.
281 Compared to the reference period, the mean annual precipitation decreased by 11.73%
282 (6.36%-15.69%) and 10.64% (5.88%-16.7%) on average in period-2 and period-3,
283 respectively. From period-2 to period-3, the change of mean annual precipitation was slight
284 (increased by 1.32% on average) with a decrease of 2.45%-5.87% in four catchments and an
285 increase in the remaining catchments (0.35%-8.29%). The variability of annual P also
286 decreased as indicated by the reductions of C_v values during period-2 and period-3 (Fig. 7a).
287 In contrast to annual P , the reductions of mean annual Q , SSY , SC and C_s were clearly more
288 evident. With respect to the reference period, the reduction was 34.41% (9.45%-54.72%),
289 48.02% (17.98%-67.61%), 24.20% (-9.93%-47.77%) and 39.31% (4.64%-63.5%) for Q , SSY ,

290 SC and C_s during period-2, and the decreasing rate was even more in period-3 with values of
291 64.82% (36.72%-84.19%), 88.23% (64.94%-97.64%), 67.81% (17.28%-91.12%) and 85.85%
292 (63.51%-96.97%), respectively. C_v of annual Q increased in eight catchments, with the
293 remaining ones showing decreasing trends (Fig. 7b), while C_v values for SSY , SC and C_s
294 increased in all catchments (Figs 7c-7e). The above results indicate substantially different
295 behaviors of the changes among precipitation, streamflow and sediment load.

296 **3.3 Quantitative attribution of sediment yield decline**

297 The effects of precipitation change and LUCC on sediment yield reductions in period-2 and
298 period-3 were quantified using Eqs. (2-6) and the results are shown in Fig. 8. The form of
299 Eq. (6) during the reference period is shown in Table 3. The analysis showed that both
300 decreased precipitation and increased area treated with erosion control measures
301 contributed to the observed sediment load reduction, and that LUCC played the major role.
302 On average, LUCC and precipitation change contributed 74.39% and 25.61%, respectively,
303 to sediment load reduction from the reference period to period-2, with their respective
304 contributions to sediment load reduction from the reference period to period-3 being 88.67
305 and 11.33%. The effect of LUCC in period-3 was greater than in period-2 as the land
306 use/cover (see Figs. 4-5) and vegetation coverage (see Fig. 6) had undergone substantial
307 changes due to the ecological restoration campaigns launched during period-3. From
308 period-2 to period-3, the contribution of precipitation was negative for sediment yield
309 reduction in eleven catchments where the annual precipitation slightly increased and thus
310 the contribution of LUCC was larger than 100% (Fig. 8c). In the remaining four catchments,
311 the average contribution of LUCC increased to 83.96%.

312 In broad terms there are two factors that govern annual sediment yield of a catchment:
313 precipitation and landscape properties (soil, topography and vegetation). Precipitation is the
314 primary driver of runoff and, therefore, directly influences the sediment transport capacity
315 of streamflow and sediment yield at the catchment scale. Higher precipitation means higher
316 streamflow, which is the immediate driver of erosion and sediment transport. Landscape
317 properties not only have an impact on the volume or intensity of streamflow, but also
318 determine the erodibility of the soil. Correlations between the potential factors
319 (precipitation, percentage area of afforestation, pasture plantation, terracing, check-dams
320 and construction land, and LAI) and sediment yield change between different stages (see
321 Table 4) showed that check-dam construction was the dominant factor for sediment yield
322 reduction from reference period to period-2. Pasture plantation and check-dam construction
323 acted as the dominant factors for sediment yield from reference period to period-3. The
324 increase of precipitation mitigated the reduction of sediment yield to some degree from
325 period-2 to period-3.

326 Based on the above results, the variation of *SSY* mainly depended on precipitation in the
327 reference period before LUCC took effect and any spatial patterns of *SSY* in the catchments
328 were controlled by differences in annual precipitation and land surface conditions. During
329 the validation period (period-2 and period-3) when increased LUCC had taken effect, *SSY*
330 decreased considerably. The decrease of precipitation was insignificant and LUCC
331 contributed over 70% of the sediment yield reduction. In this case, the temporal changes of
332 *SSY* depended more on the fraction of treated surface area and precipitation possibly played
333 a secondary role. The spatial pattern of the impacts of precipitation on sediment yield was

334 dependent on the landscape properties among catchments. Guided by this framework, data
335 were next analysed to generate separate spatial and temporal patterns constituting
336 respective components of the spatio-temporal patterns.

337 **3.4 Spatial-temporal pattern of the impacts of precipitation on sediment yield**

338 The regression equations of $\sqrt{SSY} = aP + b$ are shown in Table 3. The spatial distributions
339 of precipitation-sediment relationships during the three stages are shown in Fig. 9. During
340 the reference period, the correlation between precipitation and sediment yield was
341 significant in eleven catchments ($p < 0.05$) with the coefficient of determination (R^2) ranged
342 from 0.48 to 0.87 (Table 3). Furthermore, the precipitation-sediment yield relationship
343 varied from catchment to catchment and showed a spatial pattern. The correlation
344 coefficient between precipitation and sediment yield was greater for catchments in the
345 northwestern part with average R^2 value of 0.75 and p value of 0.007 compared to those in
346 the southeastern part where the average R^2 and p values were 0.48 and 0.059, respectively
347 (Table 3). Based on the slopes of the regression equations between annual precipitation and
348 sediment yield, the fourteen catchments were classified into four groups (Group-1: $a > 0.3$,
349 Group-2: $0.2 < a < 0.3$, Group-3: $0.1 < a < 0.2$ and Group-4: $0 < a < 0.1$), which indicate that the
350 sediment production capability of annual precipitation is different among the catchments
351 (Fig. 9a). The four catchments in the northwestern part (#1-3 and 5) had the greatest
352 regression slopes of $a > 0.3$ (Group-1) and the Shiwang catchment had the lowest regression
353 slope of 0.07 (Group-4). Most of the catchments in the southeastern part were in the second
354 group of $0.2 < a < 0.3$. Overall, the regressed equations were significant for most of the
355 catchments, and were suitable for estimating the relative contributions of LUCC and

356 precipitation variability to sediment yield changes.

357 Compared to the reference period, the correlation between precipitation and sediment
358 yield during the period-2 decreased in the catchments, as indicated by lower R^2 values in
359 Table 3. The slopes of the regression lines in the period-2 decreased in most of the
360 catchments with respect to the reference period, except in Huangfu, Gushan and Kuye
361 catchments which increased slightly. Furthermore, the spatial patterns of the
362 precipitation-sediment yield relationship during these two periods were somewhat different
363 (Figs. 9a and 9b). From the reference period to period-2, Jialu catchment moved from
364 Group-1 to Group-2 and five catchments moved from Group-2 to Group-3.

365 During period-3, the correlation between precipitation and sediment yield was weaker
366 compared to the reference period and period-2 (Table 3). The relationships between
367 precipitation and sediment yield were not significant in all the catchments (Table 3). The
368 slopes of the regression lines during period-3 decreased sharply (Table 3). Six catchments
369 (five in the north-western part and one in the south-eastern part) had negative regression
370 slopes (Fig. 9c). This result indicates that the sediment production capability of annual
371 precipitation decreased greatly during period-3, and the increase of precipitation amount in
372 some catchments did not lead to increased sediment yield. Furthermore, the spatial patterns
373 of precipitation-sediment relationship during period-3 were clearly different from those
374 during the reference period and period-2 (compare Fig. 9c against Figs. 9a-9b). There were
375 only three groups with two catchments having regression slopes of $0.1 < a < 0.2$, six
376 catchments having regression slopes of $0.1 < a < 0.2$ and six catchments having negative
377 regression slopes.

378 The aforementioned analysis of the precipitation-sediment yield relationship in
379 different periods clearly indicates that the impacts of precipitation on sediment yield
380 declined with time. The impacts were different among catchments, with a clear spatial
381 pattern. The effects of precipitation on the sediment yield were greater in the north-western
382 part compared to those in the south-eastern part. The decreased effects of precipitation on
383 sediment yield with time were consistent with the significant reductions of sediment
384 coefficient (Table 2) and the decreased contribution of precipitation to sediment load
385 reduction (25.61% and 11.33% in period-2 and period-3, respectively). During period-2,
386 the LUCC were mainly induced by SWCM, especially engineering measures. During
387 period-3, the combined effects of substantial vegetation cover and conservation measures
388 further weakened the effects of precipitation on sediment load reduction.

389 **3.5 Spatial-temporal pattern of the impacts of land use/cover on sediment yield**

390 In order to quantify the effects of SWCM on sediment load reduction, the relationships
391 between the decadal sediment coefficient and the fraction of area treated with erosion control
392 measures in the 15 catchments were analysed and the results are presented in Table 5. The
393 decadal sediment coefficient (\overline{SC}) decreased linearly with the fraction of treated land surface
394 area (A_c) in all catchments:

$$395 \quad \overline{SC} = -mA_c + n \quad (7)$$

396 The correlations were significant in eleven catchments ($p < 0.05$) with R^2 ranging from
397 0.78 to 0.99 (Table 5). The effects of SWCM on sediment load change show a spatial pattern.
398 The correlation between sediment coefficients and conservation measures were stronger in
399 catchments located in the north-western part compared to that in the south-eastern part (Table

400 5). Based on the slope of the regression equation between the sediment coefficient and
401 fraction of the treated area, the catchments were classified into three groups in Fig. 10
402 (Group-1: $0.8 < m < 1.2$, Group-2: $0.4 < m < 0.8$ and Group-3: $0 < m < 0.4$), which indicated that the
403 degree of sediment load impacted by conservation measures was different among the
404 catchments. The average m value was 0.73 and 0.37 for the catchments in the north-western
405 and south-eastern part, respectively. Half of the catchments in the north-western part were in
406 Group-1 and the other half were in Group-2, whereas six of the eight catchments in the
407 south-eastern part were in Group-3 with lowest regression slope.

408 **3.6 Discussion**

409 Differences in catchment characteristics, including land use/cover, soil properties and
410 topography, as well as precipitation characteristics, are clearly the reason for the spatial
411 patterns in the precipitation-sediment yield relationship (Morera et al., 2013; Mutema et al.,
412 2015). The lower vegetation cover was the main reason for the greater effects of
413 precipitation on sediment yield in the northwestern part. In order to fully explore this, the
414 mapping of information of catchment characteristics into sediment yield models and
415 simulations under different climate scenarios would be needed (Ma et al., 2014; Achete et
416 al., 2015). In this context, the inter-annual and intra-annual patterns of variability of
417 precipitation, including the distribution of storm events, may also contribute to the
418 observed spatial patterns of precipitation-sediment yield relationship.

419 As LUCC took effect during period-2 and period-3, and despite the much reduced role
420 of precipitation in driving changes in sediment yield, within-year temporal rainfall patterns
421 did play an important role in the observed changes of sediment yield, given that most of the

422 sediment yield was produced during a few key storm events. The correlation between
423 sediment yield and storm events with daily precipitation amount larger than 20 mm
424 (including storm numbers, precipitation amount of storms) in the CSHC region during
425 different decades were investigated (see Table 6). The analysis showed that the sediment
426 yield was significantly correlated with storm numbers in the 1960s, 1970s and 1980s
427 ($p<0.05$), and precipitation amount of storms in the 1960s and 1970s ($p<0.05$). This result
428 indicated the critical role of storm events in sediment yield, especially during the periods
429 before substantial LUCC took effect.

430 Looking into this in more detail and taking the Yanhe catchment as an example, the
431 precipitation amount during the rainy season (May-October when sediment load was
432 measured) in 2003 and 2004 was 514.31 mm and 389.05 mm, respectively, whereas the
433 sediment load in 2004 (2427.37×10^4 t) was about over four times of that in 2004
434 (590.04×10^4 t). As shown in Fig. 11, there were six days with precipitation amounts over
435 20 mm and the maximum daily precipitation amount on 25th August was 27.85 mm in 2003,
436 and the values in 2004 were five days and 46.34 mm on 10th August. Furthermore, heavy
437 rainfall events were distributed in every month in 2003, whereas they were concentrated in
438 July and August in 2004. There were five evident peaks of sediment load with the sum of
439 1646.24×10^4 t (67.82% of annual total) in 2004, especially the one on 10th August
440 produced 784.53×10^4 t sediment load (32.32% of annual total) (Fig. 11b). In contrast, there
441 were three peaks of sediment load in 2003, and the maximum value was only 139.97×10^4 t
442 (Fig. 11a). Therefore, apart from annual precipitation amounts, within-year rainfall patterns
443 should also be considered when investigating the effects of precipitation on

444 temporal-spatial changes of streamflow and sediment load.

445 The sediment load reductions in the CSHC region were primarily caused by the LUCC
446 and the implementation of SWCM. The cropland area decreased 9733.91 km² (8.73% of
447 region area) and the forestland area increased 7662.50 km² (6.87% of region area) in the
448 region from 1975 to 2010. Most of the increase in forestland area was converted from
449 cropland area induced by the GFG or reforestation project. As a result of the land use change,
450 vegetation cover increased greatly and it substantially contributed to the decreases of runoff
451 and sediment production. The SWCMs, such as afforestation and engineering measures were
452 the major interventions in the study area to reduce the runoff-sediment generation from
453 precipitation and retain streamflow and sediment load within the catchment. Establishing
454 perennial vegetation cover was considered as one of the most effective measures to stabilize
455 soils and minimize erosion (Farley et al., 2005; Liu et al., 2014). It was reported that both
456 runoff coefficient and sediment concentration of catchments in the LP decreased significantly
457 and linearly with the vegetation cover (Wang et al., 2016). The engineering structures mainly
458 included creation of terrace and building of check-dams and reservoirs, which reduced flood
459 peaks and stored water and sediment within the catchment. There were about 59, 874
460 check-dams in the region which trapped about 9842×10^4 t of sediment per year
461 (approximately 19% of annual sediment yield) during the past six decades (Yao et al., 2011).
462 Over time, the effectiveness of engineering measures decreased as they progressively filled
463 with sediments, and vegetation restoration played a greater role in controlling soil erosion.

464 **4 Conclusions**

465 Through analyses of hydrological and sediment transport data, this study has shown that

466 long-term decreasing trends in sediment loads across fifteen large sub-catchments located
467 in the CSHC region for the period 1961-2011. The study was particularly aimed at
468 extracting spatio-temporal patterns of sediment yield and attributing these patterns to the
469 broad hydro-climatic and landscape controls. The effects of precipitation variability and
470 land use/cover changes on sediment yield were investigated in detail.

471 Over the study period, the total area undergoing erosion control treatment went up
472 from only 4% to over 30%. This included to decrease of cropland by 27%, increase of
473 forestland by 53% and grassland by 4% from 1975-2010. Over the same period annual
474 precipitation decreased by not more than 10%. As a result of the erosion control measures,
475 there were major reductions in streamflow (65%), sediment yield (88%), sediment
476 concentration (68%) and sediment efficiency, i.e., annual sediment yield/annual
477 precipitation (86%) over the entire 50-year period.

478 The observed data in the 15 study catchments also exhibited interesting
479 spatio-temporal patterns in sediment yield. The study attempted to separate the relative
480 contributions of annual precipitation and LUCC to these spatio-temporal patterns. Before
481 LUCC took effect, the data indicates a linear relationship between square root of annual
482 sediment yield and annual precipitation in all 15 catchments, with highly variable slopes of
483 the relationship between the catchments, which exhibited systematic spatial patterns, in
484 spite of some scatter. As LUCC increased and took effect, the scatter increased and the
485 slopes of the sediment yield vs precipitation relationship became highly variable and lost
486 any predictive power. The study then looked at the controls on sediment coefficient instead
487 of sediment yield, thus eliminating the effect of precipitation and enabling a direct focus on

488 landscape controls. The results of this analysis found that sediment coefficient was heavily
489 dependent on the area under land use/cover treatment, exhibiting a linear decreasing
490 relationship. Even here, there was a considerable variation in the slope of the relationship
491 between the 15 catchments, which exhibited a systematic spatial pattern.

492 Preliminary analyses presented in this study suggest that much of the sediment yield in
493 the LP may be caused during only a few major storms. Therefore, the seasonality and
494 intra-annual variability of precipitation may play important roles in annual sediment yield,
495 which may also explain the spatial patterns of sediment yield and the effects of the various
496 LUCC. Also, the precipitation threshold for producing sediment yield would have increased
497 greatly as a result of SWCM and vegetation restoration in the LP. Exploration of these
498 questions in detail will require a more physically based model that can account for fine
499 scale rainfall variability and catchment characteristics. This is the next immediate step in
500 our investigations, and will be reported on in the near future.

501

502 **Acknowledgements**

503 This research was funded by the National Key Research and Development Program of China
504 (no. 2017YFC0501602), the National Natural Science Foundation of China (no. 41471094),
505 the Chinese Academy of Sciences (no. GJHZ 1502) and the Youth Innovation Promotion
506 Association CAS (no. 2016040). We thank the Ecological Environment Database of Loess
507 Plateau, the Yellow River Conservancy Commission, and the National Meteorological
508 Information Center for providing the hydrological and meteorological data. We thank the
509 three anonymous reviewers for their valuable and detailed comments which greatly improve

510 the quality of this manuscript.

511

512 **References**

513 Achete, F.M., van der Wegen, M., Roelvink, D., and Jaffe, B.: A 2-D process-based model

514 for suspended sediment dynamics: a first step towards ecological modeling, *Hydrol.*

515 *Earth Syst. Sci.*, 19, 2837-2857, 2015.

516 Beechie, T. J., Sear, D.A., Olden, J.D., Pess, G.R., Buffington, J.M., Moir, H., Roni, P., and

517 Pollock, M.M.: Process-based principles for restoring river ecosystems, *Bioscience*, 60,

518 209-222, 2010.

519 Chen, Y.P., Wang, K.B., Lin, Y.S., Shi, W.Y., Song, Y., and He, X.H.: Balancing green and

520 grain trade, *Nat. Geosci.*, 8, 739-741, 2015.

521 Cohen, S., Kettner, A.J., and Syvitski, J.P.M.: Global suspended sediment and water

522 discharge dynamics between 1960 and 2010: continental trends and intra-basin

523 sensitivity, *Glob. Planet. Chang.*, 115, 44-58, 2014.

524 Farley, K.A., Jobbágy, E.G., and Jackson, R.B.: Effects of afforestation on water yield: a

525 global synthesis with implications for policy, *Glob. Chang. Biol.*, 11, 1565-1576, 2005.

526 Hirsch, R.M., Slack, J.R., and Smith, R.A.: Techniques of trend analysis for monthly water

527 quality data, *Water Resour. Res.*, 18, 107-121, 1982.

528 Kendall, M.G.: *Rank Correlation Measures*, Charles Griffin, London, UK, 1975.

529 Liu, X.Y., Yang, S.T., Dang, S.Z., Luo, Y., Li, X.Y., and Zhou X.: Response of sediment

530 yield to vegetation restoration at a large spatial scale in the Loess Plateau, *Sci. China*

531 *Tech. Sci.*, 57, 1482-1489, 2014.

532 Mann, H.B.: Nonparametric tests against trend, *Econometrica*, 13(3), 245-259, 1945.

533 Ma, X., Lu, X.X., van Noordwijk, M., Li, J.T., and Xu, J.C.: Attribution of climate change,
534 vegetation restoration, and engineering measures to the reduction of suspended sediment
535 in the Kejie catchment, southwest China, *Hydrol. Earth Syst. Sci.*, 18, 1979-1994, 2014.

536 McVicar, T.R., Li, L.T., Van Niel, T.G., Zhang, L., Li, R., Yang, Q.K., Zhang, X.P., Mu, X.M.,
537 Wen, Z.M., Liu, W.Z., Zhao, Y.A., Liu, Z.H, and Gao, P.: Developing a decision support
538 tool for China's re-vegetation program: simulating regional impacts of afforestation on
539 average annual streamflow in the Loess Plateau, *For. Ecol. Manag.*, 251, 65-81, 2007.

540 Miao, C.Y., Ni, J.R., and Borthwick, A.G.L.: Recent changes of water discharge and
541 sediment load in the Yellow River basin, China, *Prog. Phys. Geogr.*, 34, 541-561, 2010.

542 Miao, C.Y., Ni, J.R., Borthwick, A.G.L, and Yang, L.: A preliminary estimate of human and
543 natural contributions to the changes in water discharge and sediment load in the Yellow
544 River, *Glob. Planet. Chang.*, 76, 196-205, 2011.

545 Milliman, J.D., Farnsworth, K.L., Jones, P.D., Xu, K.H., and Smith, L.C.: Climatic and
546 anthropogenic factors affecting river discharge to the global ocean, 1951-2000, *Glob.*
547 *Planet. Chang.*, 62, 187-194, 2008.

548 Milly, P.C.D., Dunne, K.A., and Vecchia, A.V.: Global pattern of trends in streamflow and
549 water availability in a changing climate, *Nature*, 438, 347-350, 2005.

550 Morera, S.B., Condom, T., Vauchel, P., Guyot, J.-L., Galvez, C., and Crave, A.: Pertinent
551 spatio-temporal scale of observation to understand suspended sediment yield control
552 factors in the Andean region: the case of the Santa River (Peru), *Hydrol. Earth Syst. Sci.*,
553 17, 4641-4657, 2013.

554 Mutema, M., Chaplot, V., Jewitt, G., Chivenge, P., and Blöschl, G.: Annual water, sediment,
555 nutrient, and organic carbon fluxes in river basins: A global meta-analysis as a function
556 of scale, *Water Resour. Res.*, 51, doi:10.1002/2014WR016668, 2015.

557 Nilsson, C., Reidy, C.A., Dynesius, M., and Revenga, C.: Fragmentation and flow regulation
558 of the world's large river systems, *Science*, 308, 405-408, 2005.

559 Rustomji, P., Zhang, X.P., Hairsine, P.B., Zhang, L., and Zhao J.: River sediment load and
560 concentration responses to changes in hydrology and catchment management in the
561 Loess Plateau of China, *Water Resour. Res.*, 44, W00A04, doi:10.1029/2007WR006656,
562 2008.

563 Sen, P.K., 1968. Estimates of the regression coefficient based on Kendall's tau, *J. Am. Stat.*
564 *Assoc.*, 63, 1379-1389.

565 Song, C.L., Wang, G.X., Sun, X.Y., Chang, R.Y., and Mao, T.X.: Control factors and scale
566 analysis of annual river water, sediments and carbon transport in China, *Sci. Rep.*,
567 6:25963, doi:10.1038/srep25963, 2016.

568 Sun, Q.H., Miao, C.Y., Duan, Q.Y., and Wang, Y.F.: Temperature and precipitation changes
569 over the Loess Plateau between 1961 and 2011, based on high-density gauge
570 observations, *Glob. Planet. Chang.*, 132, 1-10, 2015a.

571 Sun, W.Y., Song, X.Y., Mu, X.M., Gao, P., Wang, F., and Zhao, G.J.: Spatiotemporal
572 vegetation cover variations associated with climate change and ecological restoration in
573 the Loess Plateau, *Agric. For. Meteorol.*, 209, 87-99, 2015b.

574 Syvitski, J.P.M.: Supply and flux of sediment along hydrological pathways: Research for the
575 21st century, *Glob. Planet. Chang.*, 39, 1-11, 2003.

576 Syvitski, J.P.M., Vörösmarty, C.J., Kettner, A.J., and Green, P.: Impact of humans on the flux
577 of terrestrial sediment to the global coastal ocean, *Science*, 308, 376-380, 2005.

578 Walling, D.E. and Fang, D.: Recent trends in the suspended sediment loads of the world
579 rivers, *Glob. Planet. Chang.*, 39, 111-126, 2003.

580 Walling, D.E.: Human impact on land-ocean sediment transfer by the world's rivers,
581 *Geomorphology*, 79, 192-216, 2006.

582 Wang, H.J., Saito, Y., Zhang, Y., Bi, N.S., Sun, X.X., and Yang, Z.S.: Recent changes of
583 sediment flux to the western Pacific Ocean from major rivers in east and south-east Asia,
584 *Earth Sci. Rev.*, 108, 80-100, 2011.

585 Wang, S., Fu, B., Piao, S., Lü, Y., Philippe, C., Feng, X., and Wang, Y.: Reduced sediment
586 transport in the Yellow River due to anthropogenic changes, *Nat. Geosci.*, 9, 38-41,
587 2016.

588 Yao, W.Y., Xu, J.H., and Ran, D.C.: Assessment of Changing Trends in Streamflow and
589 Sediment Fluxes in the Yellow River Basin, Yellow River Water Conservancy Press,
590 Zhengzhou, China, 2011 (in Chinese).

591 Yue, S. and Wang, C.Y.: Applicability of pre-whitening to eliminate the influence of serial
592 correlation on the Mann-Kendall test, *Water Resour. Res.*, 38, 1068,
593 doi:10.1029/2001WR000861, 2002.

594 Zhang, B.Q., He, C.S., Burnham, M., and Zhang, L.H.: Evaluating the coupling effects of
595 climate aridity and vegetation restoration on soil erosion over the Loess Plateau in China,
596 *Sci. Total Environ.*, 539, 436-449, 2016.

597 Zhang, L., Zhao, F.F., Chen, Y., and Dixon, R.N.M.: Estimating effects of plantation

598 expansion and climate variability on streamflow for catchments in Australia, *Water*
599 *Resour. Res.*, 47, W12539, doi:10.1029/2011WR010711, 2011.

600 Zhao, G.J., Mu, X.M., Jiao, J.Y., An, Z.F., Klik, A., Wang, F., Jiao, F., Yue, X.L., Gao, P., and
601 Sun, W.Y.: Evidence and causes of spatiotemporal changes in runoff and sediment yield
602 on the Chinese Loess Plateau, *Land Degrad. Dev.*, 28, 579-590, 2017.

603 Zhao, X., Liang, S.L., Liu, S.H., Yuan, W.P., Xiao, Z.Q., Liu, Q., Cheng, J., Zhang, X.T., Tang,
604 H.R., Zhang, X., Liu, Q., Zhou, G.Q., Xu, S., Yu, K.: The global land surface satellite
605 (GLASS) remote sensing data processing system and products, *Remote Sens.*, 5,
606 2436-2450, 2013.

607

608 **Figure captions**

609 **Figure 1.** Location of the studied catchments in the Coarse Sandy Hilly Catchments
610 (CSHC) region within the Loess Plateau.

611 **Figure 2.** Spatial distribution of (a) annual precipitation (1961-2011), (b) growing season
612 leaf area index (LAI, 1982-2011), (c) soil type and (d) slope in the study area.

613 **Figure 3.** Annual precipitation, streamflow and sediment load for the whole CSHC region
614 during 1961-2011.

615 **Figure 4.** Land use and cover of the study area in (a) 1975, (b) 1990, (c) 2000 and (d)
616 2010.

617 **Figure 5.** The changes of soil and water conservation measures area and growing season
618 LAI in the study area.

619 **Figure 6.** Long-term trends in growing season LAI changes over (a) 1982-2011, (b)
620 1982-1999 and (c) 2000-2011 in the study area. Inset in each figure shows the
621 frequency distribution of the LAI trends.

622 **Figure 7.** The changes of (a) precipitation, (b) streamflow, (c) sediment yield, (d) sediment
623 concentration and (e) sediment coefficient during different stages (1961-1969,
624 1970-1999 and 2000-2011).

625 **Figure 8.** Contributions of precipitation and land use/cover to reductions of sediment load
626 from (a) reference period (P1) to period-2 (P2), (b) reference period (P1) to period-3 (P3)
627 and (c) period-2 (P2) to period-3 (P3).

628 **Figure 9.** Spatial distribution of slope a in the regression equation $\sqrt{SSY} = aP + b$ during
629 (a) reference period (1961-1969), (b) period-2 (1970-1999) and (c) period-3

630 (2000-2011). SSY is specific sediment yield, and P is precipitation.

631 **Figure 10.** Spatial distribution of slope m in the regression equation $\overline{SC} = -mA_c + n$. \overline{SC} is
632 the decadal average sediment coefficient, and A_c is the percentage of the area affected by
633 soil and water conservation measures in the catchments.

634 **Figure 11.** Daily precipitation and sediment load of the Yanhe catchment during rainy
635 season (May-October) in (a) 2003 and (b) 2004.

Table 1. Long-term hydrometeorological characteristics (1961-2011) and growing season leaf area index (LAI) (1982-2011) of the studied catchments in the Loess Plateau.

ID	Catchment	Gauging station	Slope (°)	Area (km ²)	Annual average					
					<i>P</i> (mm)	<i>Q</i> (mm)	<i>SSY</i> (t km ⁻²)	<i>SC</i> (kg m ⁻³)	<i>C_s</i> (t km ⁻² mm ⁻¹)	LAI
1	Huangfu	Huangfu	7.8	3175	388.95	36.34	11608.86	275.90	27.35	0.412
2	Gushan	Gaoshiya	9.8	1263	422.49	49.55	12398.68	189.57	25.98	0.440
3	Kuye	Wenjiachuan	6.3	8515	394.63	59.25	9099.60	114.99	21.17	0.427
4	Tuwei	Gaojiachuan	5.8	3253	402.82	97.53	4454.47	38.44	10.16	0.406
5	Jialu	Shenjiawan	10.4	1121	445.51	49.22	9645.19	142.19	20.03	0.480
6	Wuding	Baijiachuan	6.8	29662	384.32	36.39	3089.61	74.09	7.67	0.460
7	Qingjian	Yanchuan	15.9	3468	485.58	38.93	8747.17	190.57	17.35	0.626
8	Yanhe	Ganguyi	16.5	5891	516.09	34.08	6604.90	166.31	12.45	0.920
9	Shiwang	Dacun	15.2	2141	572.16	32.99	798.89	20.32	1.31	3.261
10	Qiushui	Linjiaping	13.0	1873	469.02	34.83	7818.21	185.79	15.75	0.938
11	Sanchuan	Houdacheng	14.6	4102	486.23	50.37	3444.56	53.39	6.63	1.887
12	Quchan	Peigou	14.6	1023	539.73	30.24	7492.57	192.01	13.68	0.934
13	Xinshui	Daning	14.0	3992	529.96	29.22	3004.96	86.81	5.23	1.752
14	Zhouchuan	Jixian	15.3	436	530.06	30.13	4951.15	107.99	8.55	1.165
15	CSHC	Toudaoguai and Longmen	10.5	129654	437.27	33.30	3988.04	102.42	8.73	0.765

Table 2. Mann-Kendall trend analysis results for the annual precipitation (P), streamflow (Q), specific sediment yield (SSY), sediment concentration (SC), sediment coefficient (C_s) during 1961-2011.

ID	Catchment	P		Q		SSY		SC		C_s	
		Z	β (mm yr ⁻¹)	Z	β (mm yr ⁻¹)	Z	β (t km ⁻² yr ⁻¹)	Z	β (kg m ⁻³ yr ⁻¹)	Z	β (t km ⁻² mm ⁻¹ yr ⁻¹)
1	Huangfu	-0.57 ^{ns}	-0.52	-4.82***	-0.99	-4.50***	-323.24	-1.97*	-2.58	-4.71***	-0.80
2	Gushan	-0.78 ^{ns}	-1.16	-5.02***	-1.47	-4.90***	-398.82	-3.75***	-3.92	-5.15***	-0.87
3	Kuye	-0.49 ^{ns}	-0.37	-5.98***	-1.66	-5.41***	-288.83	-4.61***	-3.22	-5.60***	-0.63
4	Tuwei	-0.24 ^{ns}	-0.27	-7.88***	-1.57	-5.20***	-130.34	-4.37***	-0.98	-5.59***	-0.30
5	Jialu	0.19 ^{ns}	0.26	-7.55***	-1.42	-5.36***	-298.10	-3.80***	-3.89	-5.60***	-0.69
6	Wuding	-0.39 ^{ns}	-0.37	-6.60***	-0.54	-4.55***	-79.19	-3.33***	-1.35	-4.94***	-0.20
7	Qingjian	-0.73 ^{ns}	-0.56	-2.06*	-0.24	-3.01**	-138.54	-3.09**	-3.53	-2.73**	-0.30
8	Yanhe	-1.19 ^{ns}	-1.17	-3.22**	-0.34	-3.36***	-115.18	-3.30***	-3.07	-3.10**	-0.22
9	Shiwang	-1.20 ^{ns}	-1.50	-4.01***	-0.61	-6.26***	-26.47	-5.43***	-0.69	-6.12***	-0.04
10	Qiushui	-0.28 ^{ns}	-0.35	-5.80***	-0.97	-6.98***	-290.44	-5.00***	-4.00	-5.98***	-0.55
11	Sanchuan	-1.43 ^{ns}	-1.71	-6.09***	-0.96	-5.35***	-108.69	-5.13***	-1.60	-5.99***	-0.21
12	Quchan	-0.94 ^{ns}	-1.14	-3.23**	-0.42	-3.65***	-173.16	-3.72***	-4.12	-3.46***	-0.29
13	Xinshui	-2.37*	-2.71	-5.57***	-0.70	-5.92***	-106.30	-3.77***	-1.92	-5.60***	-0.19
14	Zhouchuan	-2.21*	-2.48	-7.20***	-0.79	-5.86***	-183.49	-6.73***	-4.70	-7.12***	-0.35
15	CSHC	-0.67 ^{ns}	-0.55	-5.91***	-0.85	-5.70***	-131.52	-4.26***	-2.06	-5.67***	-0.27

^a ***, ** and * indicate the significance levels of 0.001, 0.01 and 0.05, respectively. ns indicates the significance levels exceeds 0.05.

Table 3. The linear regression equations between square root of specific sediment yield and annual precipitation ($\sqrt{SSY} = aP + b$) during three stages (1961-1969, 1970-1999 and 2000-2011).

ID	Catchment	Reference period (1961-1969)			Period-2 (1970-1999)			Period-3 (2000-2011)		
		Regression equation	R^2	p	Regression equation	R^2	p	Regression equation	R^2	p
1	Huangfu	$y = 0.341x + 12.041$	0.78	0.002	$y = 0.397x - 11.454$	0.40	0.000	$y = 0.135x + 5.842$	0.12	0.277
2	Gushan	$y = 0.349x + 8.237$	0.84	0.001	$y = 0.354x - 5.627$	0.37	0.000	$y = 0.076x + 10.415$	0.09	0.344
3	Kuye	$y = 0.323x + 9.939$	0.67	0.007	$y = 0.325x - 3.904$	0.35	0.001	$y = 0.037x + 8.208$	0.03	0.564
4	Tuwei	$y = 0.218x + 12.635$	0.87	0.000	$y = 0.188x + 1.648$	0.22	0.008	$y = -0.030x + 27.644$	0.03	0.613
5	Jialu	$y = 0.382x + 6.976$	0.78	0.004	$y = 0.222x + 11.867$	0.13	0.049	$y = 0.072x + 7.131$	0.03	0.616
6	Wuding	$y = 0.174x + 20.544$	0.53	0.027	$y = 0.151x + 7.546$	0.26	0.004	$y = 0.107x - 1.511$	0.17	0.182
7	Qingjian	$y = 0.232x + 20.923$	0.48	0.040	$y = 0.173x + 29.319$	0.16	0.027	$y = 0.096x + 8.344$	0.05	0.522
8	Yanhe	$y = 0.243x + 0.741$	0.39	0.070	$y = 0.126x + 32.699$	0.16	0.031	$y = 0.006x + 39.338$	0.00	0.973
9	Shiwang	$y = 0.070x + 10.935$	0.27	0.150	$y = 0.079x - 7.837$	0.24	0.006	$y = -0.007x + 9.426$	0.01	0.769
10	Qiushui	$y = 0.257x + 30.738$	0.60	0.014	$y = 0.239x - 2.814$	0.29	0.002	$y = -0.111x + 72.39$	0.06	0.448
11	Sanchuan	$y = 0.191x + 15.053$	0.36	0.089	$y = 0.174x - 9.652$	0.42	0.000	$y = -0.056x + 37.680$	0.06	0.432
12	Quchan	$y = 0.202x + 34.590$	0.72	0.016	$y = 0.132x + 29.685$	0.09	0.104	$y = -0.199x + 119.247$	0.11	0.300
13	Xinshui	$y = 0.202x - 6.593$	0.71	0.004	$y = 0.184x - 17.464$	0.53	0.000	$y = 0.015x + 16.822$	0.01	0.823
14	Zhouchuan	$y = 0.207x + 20.226$	0.33	0.090	$y = 0.245x - 31.399$	0.32	0.001	$y = -0.035x + 26.145$	0.06	0.460
15	CSHC	$y = 0.218x + 5.689$	0.70	0.005	$y = 0.174x + 2.912$	0.35	0.001	$y = 0.001x + 24.996$	0.00	0.994

Table 4. The regression models for sediment yield change (ΔSSY) in different stages.

Period	Regression model	R^2	p
Reference period vs. Period-2	$\Delta SSY = -0.135 - 0.850 \times \Delta Dam$	0.886	0.000
Reference period vs. Period-3	$\Delta SSY = -0.067 - 0.659 \times \Delta Dam - 0.081 \times \Delta Pasture$	0.928	0.023
Period-2 vs. Period-3	$\Delta SSY = -0.105 - 0.488 \times \Delta Dam + 0.058 \times \Delta P - 0.129 \times \Delta Pasture$	0.905	0.003

ΔDam and $\Delta Pasture$ are changes in percentage area of check-dams and pasture plantation, respectively. ΔP is changes of annual precipitation over the two compared periods.

Table 5. Regression equations between the decadal sediment coefficient and percentage of the area affected by soil and water conservation measures ($\overline{SC} = -mA_c + n$) in the catchments.

ID	Catchment	Regression equation	R^2	p
1	Huangfu	$y = -0.67x+45.88$	0.85	0.025
2	Gushan	$y = -0.90x+46.66$	0.82	0.034
3	Kuye	$y = -0.83x+38.32$	0.89	0.017
4	Tuwei	$y = -0.48x+19.94$	0.98	0.002
5	Jialu	$y = -1.20x+53.20$	0.97	0.002
6	Wuding	$y = -0.31x+16.92$	0.97	0.003
7	Qingjian	$y = -0.31x+24.70$	0.48	0.193
8	Yanhe	$y = -0.26x+18.54$	0.79	0.045
9	Shiwang	$y = -0.15x+3.01$	0.87	0.020
10	Qiushui	$y = -0.87x+35.69$	0.80	0.040
11	Sanchuan	$y = -0.28x+13.32$	0.78	0.046
12	Quchan	$y = -0.29x+21.02$	0.52	0.169
13	Xinshui	$y = -0.20x+8.63$	0.72	0.069
14	Zhouchuan	$y = -0.61x+17.89$	0.61	0.118
15	CSHC	$y = -0.54x+17.74$	0.99	0.000

Table 6. Pearson correlation coefficients (r) and two-tailed significance test values (p) between sediment yield and annual precipitation (P), number of storms (N_{storm}) and precipitation amount of storms (P_{storm}) during different decades of the CSHC region.

Decades	P		N_{storm}		P_{storm}	
	r	p	r	p	r	p
1960s	0.772	0.015*	0.808	0.008**	0.718	0.029*
1970s	0.266	0.458	0.714	0.020*	0.695	0.026*
1980s	0.775	0.009**	0.633	0.050*	0.527	0.117
1990s	0.865	0.001***	0.591	0.072	0.572	0.084
2000s	0.118	0.715	0.006	0.986	0.138	0.669

***, ** and * indicate the significance levels of 0.001, 0.01 and 0.05, respectively.

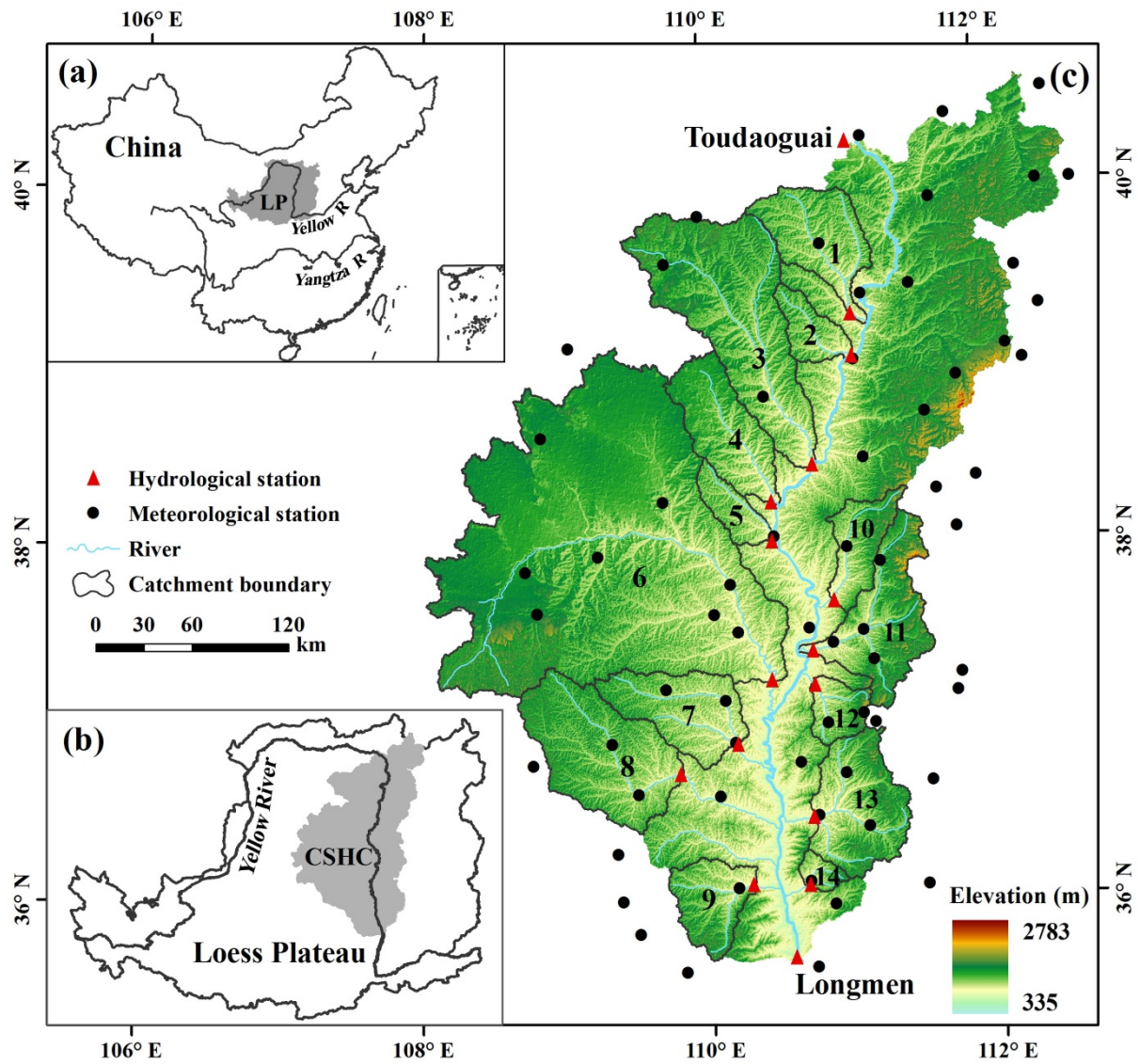


Figure 1. Location of the studied catchments in the Coarse Sandy Hilly Catchments (CSHC) region within the Loess Plateau.

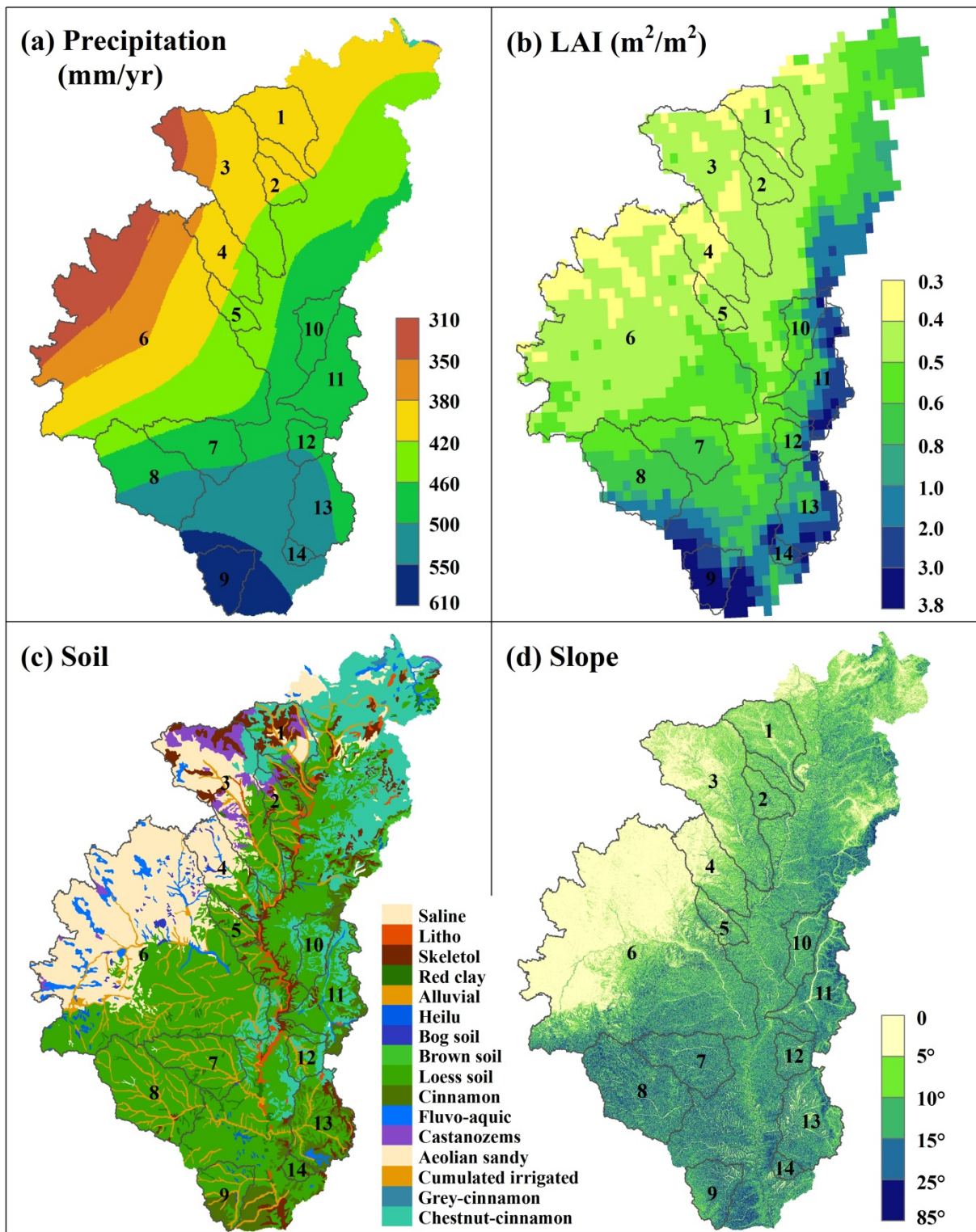


Figure 2. Spatial distribution of (a) annual mean precipitation (1961-2011), (b) growing season leaf area index (LAI, 1982-2011), (c) soil type and (d) slope in the study area.

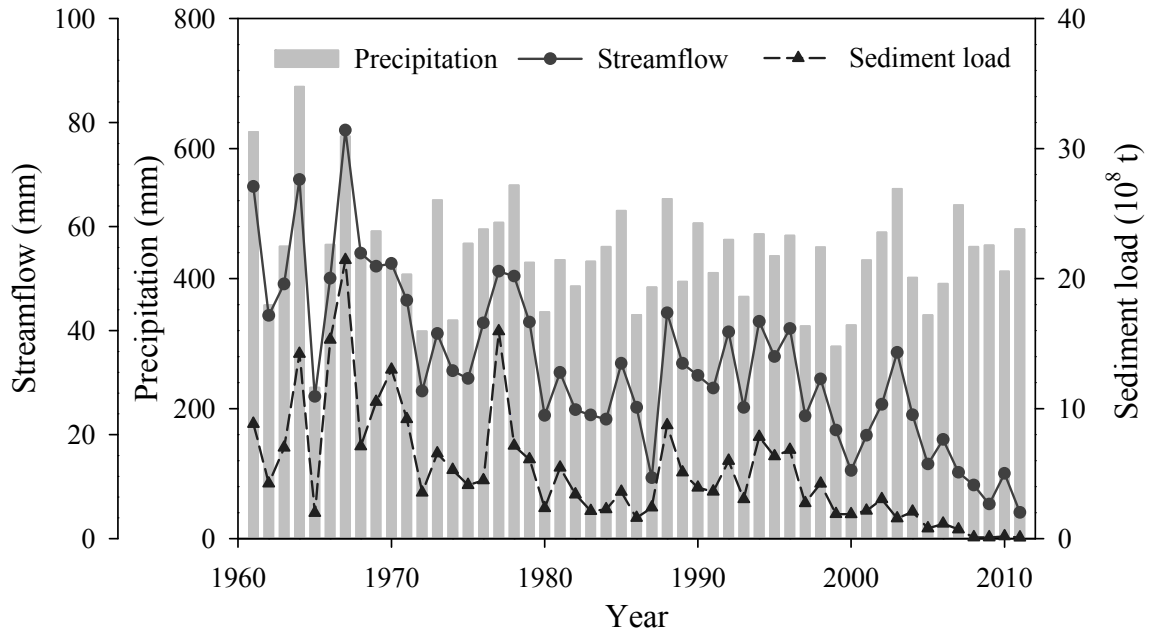


Figure 3. Annual precipitation, streamflow and sediment load for the whole CSHC region during 1961-2011.

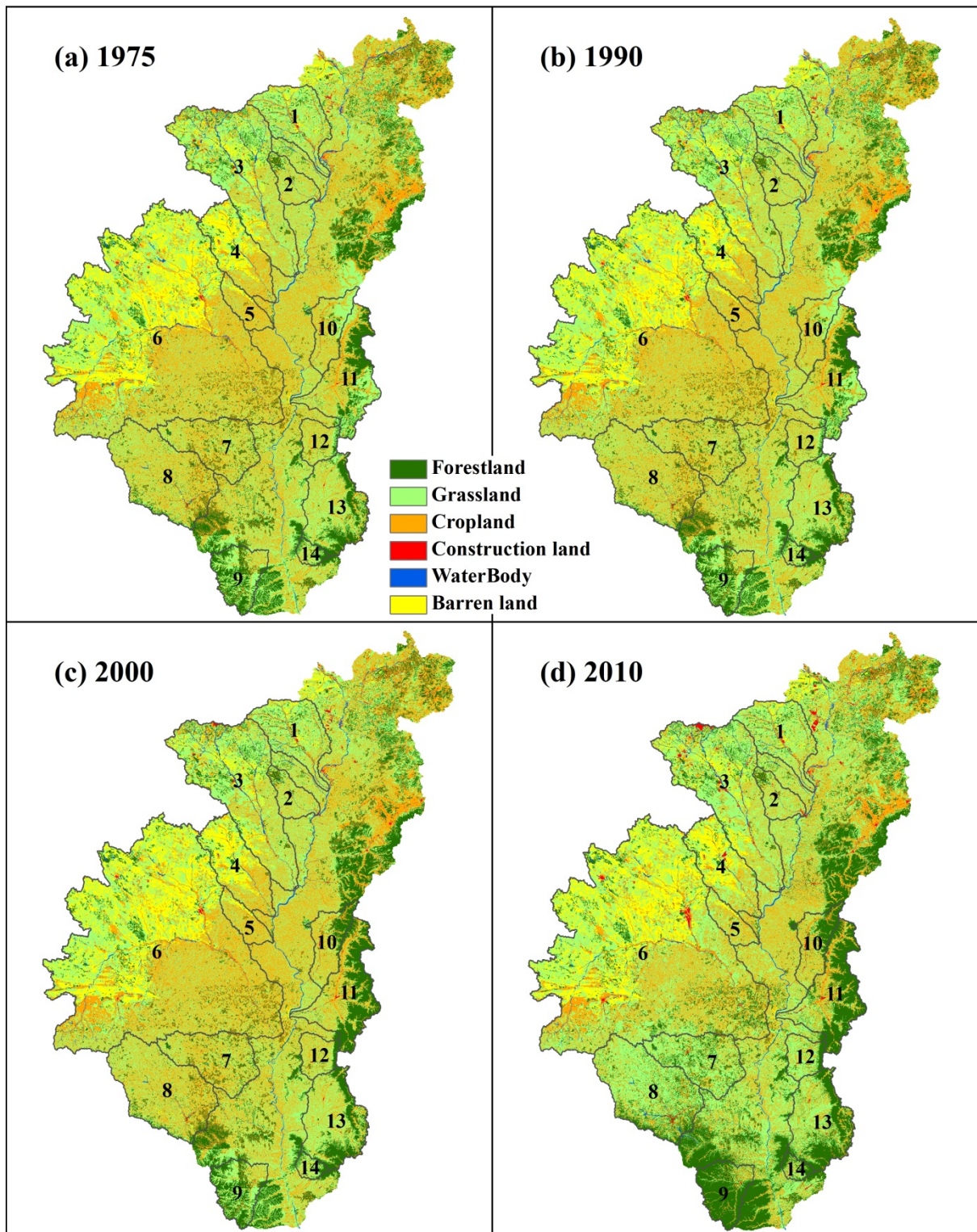


Figure 4. Land use and cover of the study area in (a) 1975, (b) 1990, (c) 2000 and (d) 2010.

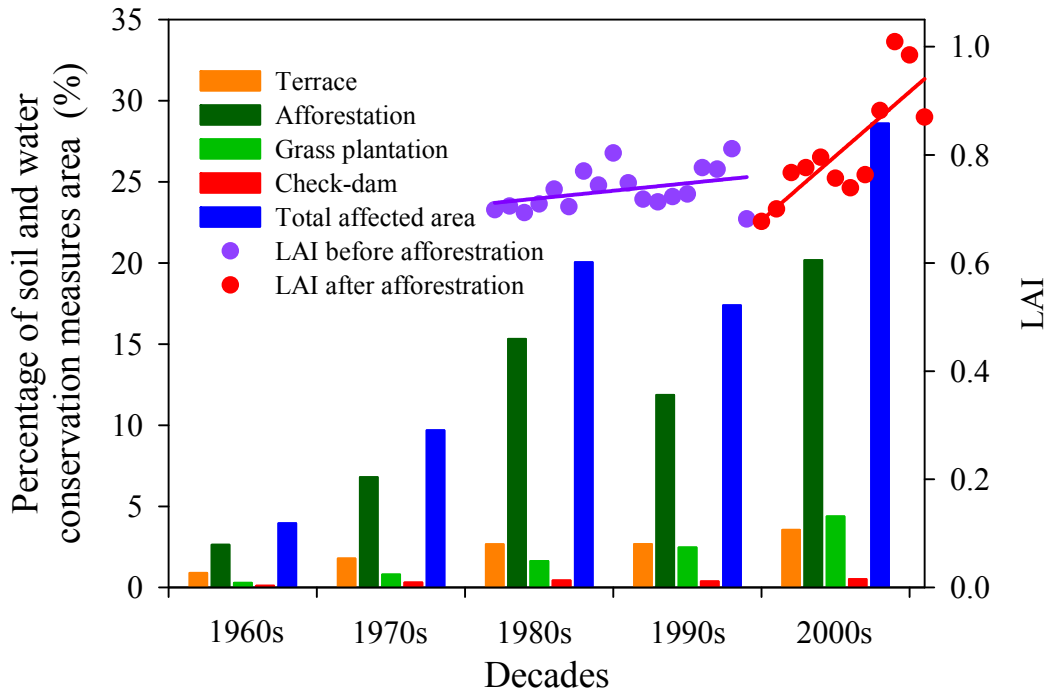


Figure 5. The changes of soil and water conservation measures area and growing season LAI in the study area.

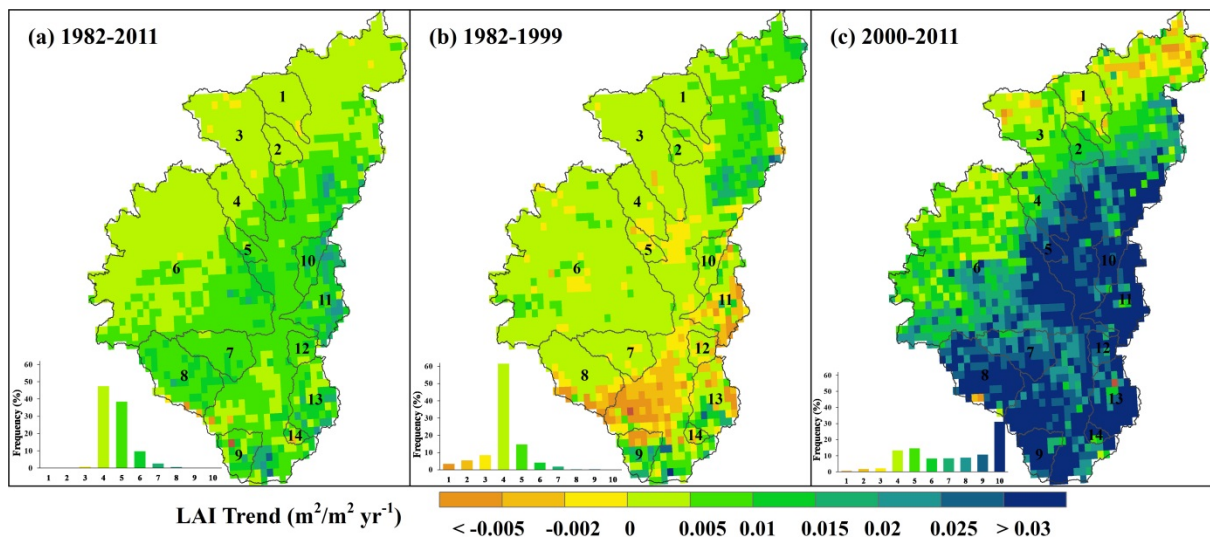
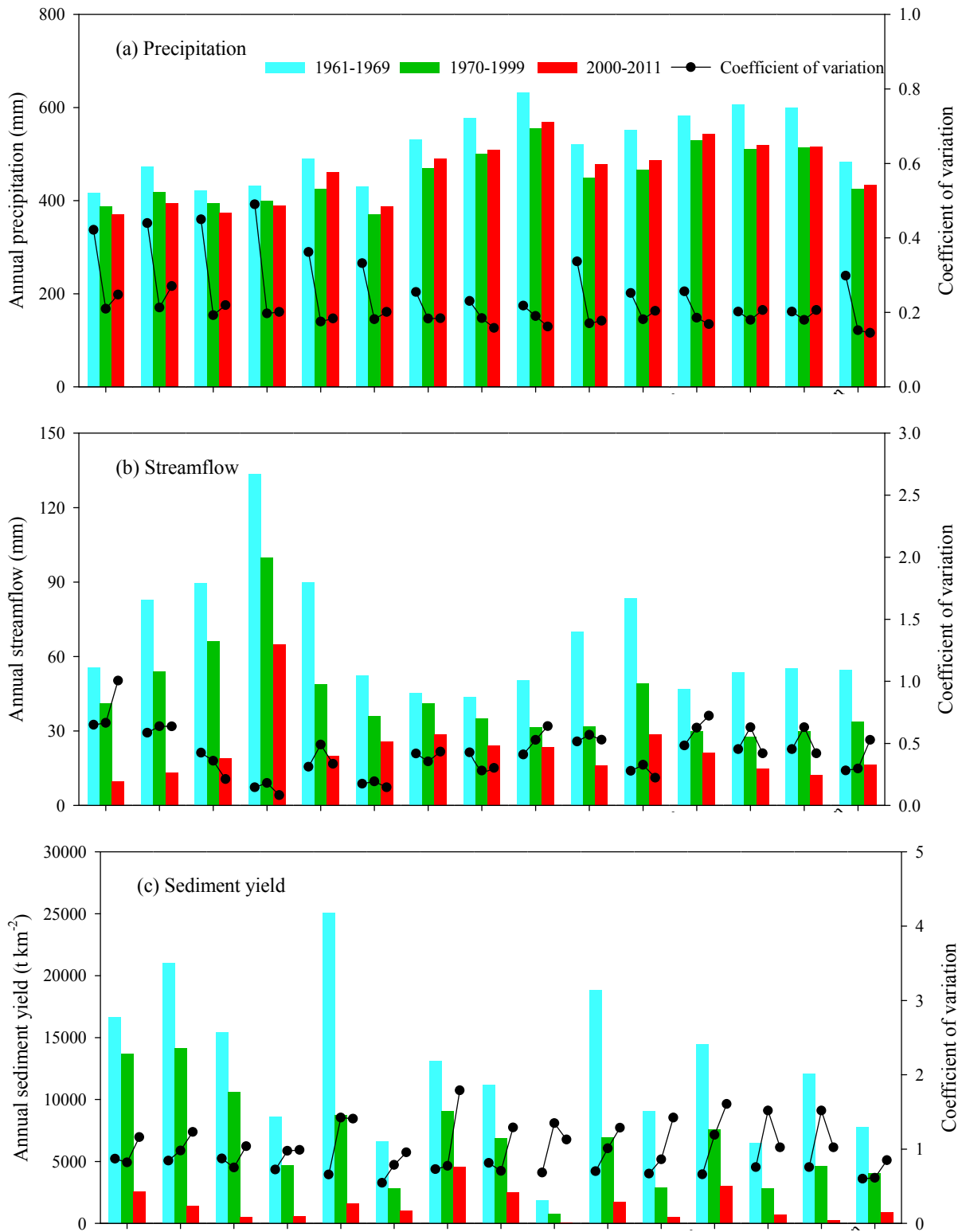


Figure 6. Long-term trends in growing season LAI changes over (a) 1982-2011, (b) 1982-1999 and (c) 2000-2011 in the study area. Inset in each figure shows the frequency distribution of the LAI trends.



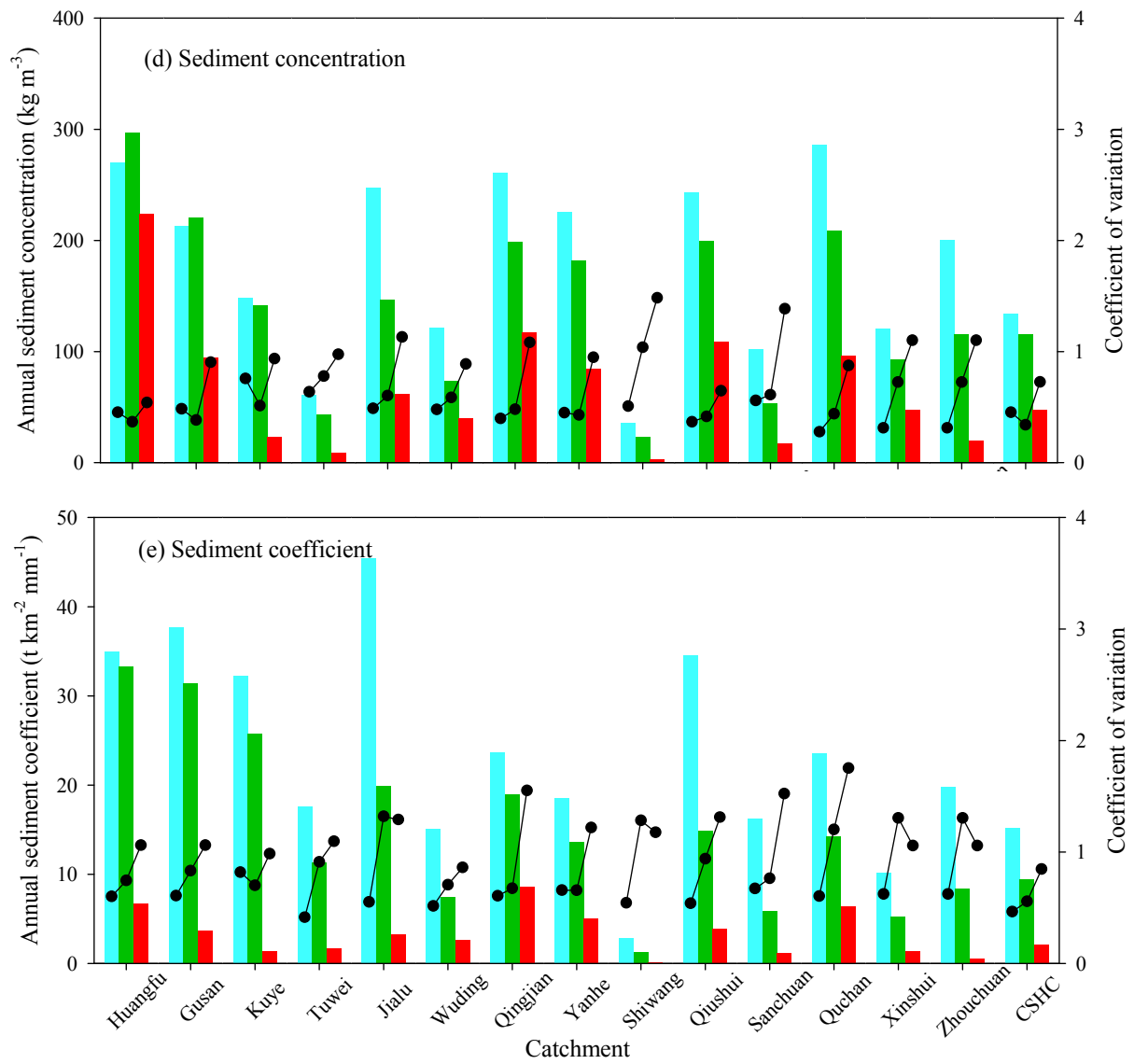


Figure 7. The changes of (a) precipitation, (b) streamflow, (c) sediment yield, (d) sediment concentration and (e) sediment coefficient during different stages (1961-1969, 1970-1999 and 2000-2011).

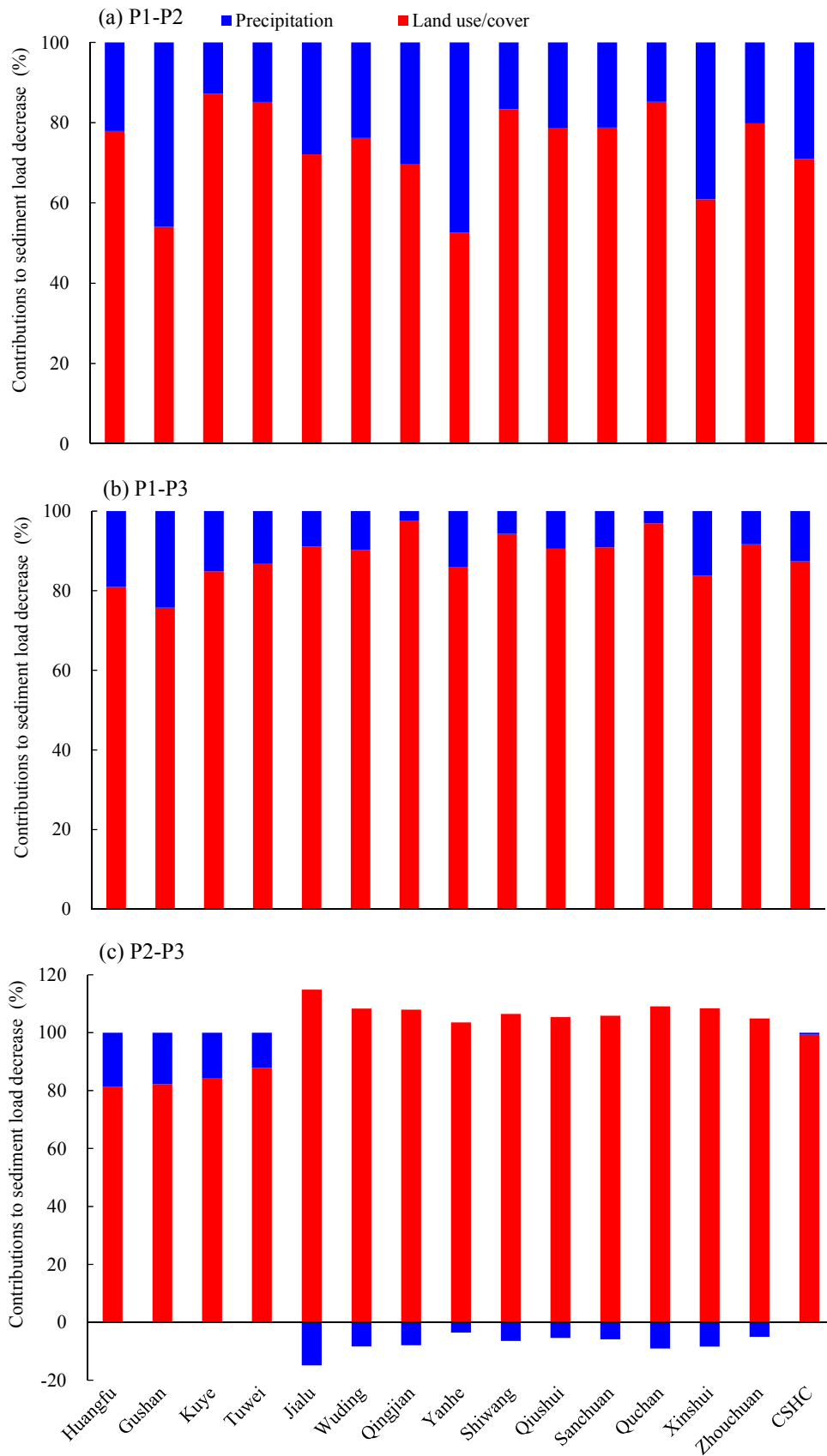


Figure 8. Contributions of precipitation and land use/cover to reductions of sediment load from (a) reference period (P1) to period-2 (P2), (b) reference period (P1) to period-3 (P3) and (c) period-2 (P2) to period-3 (P3).

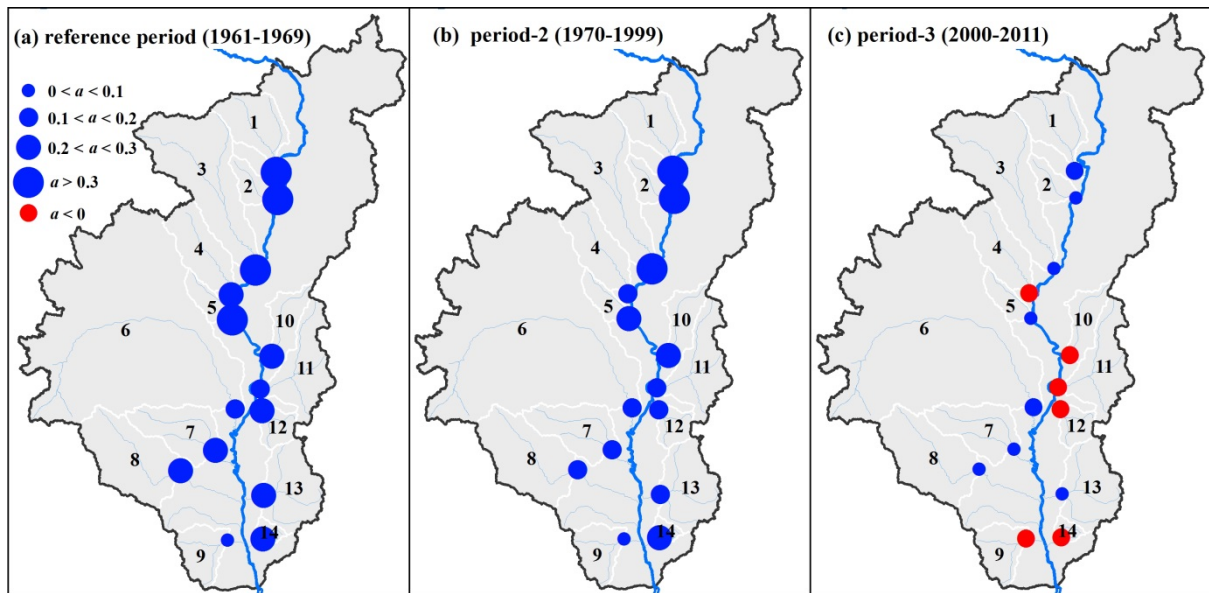


Figure 9. Spatial distribution of slope a in the regression equation $\sqrt{SSY} = aP + b$ during (a) reference period (1961-1969), (b) period-2 (1970-1999) and (c) period-3 (2000-2011). SSY is specific sediment yield, and P is precipitation.

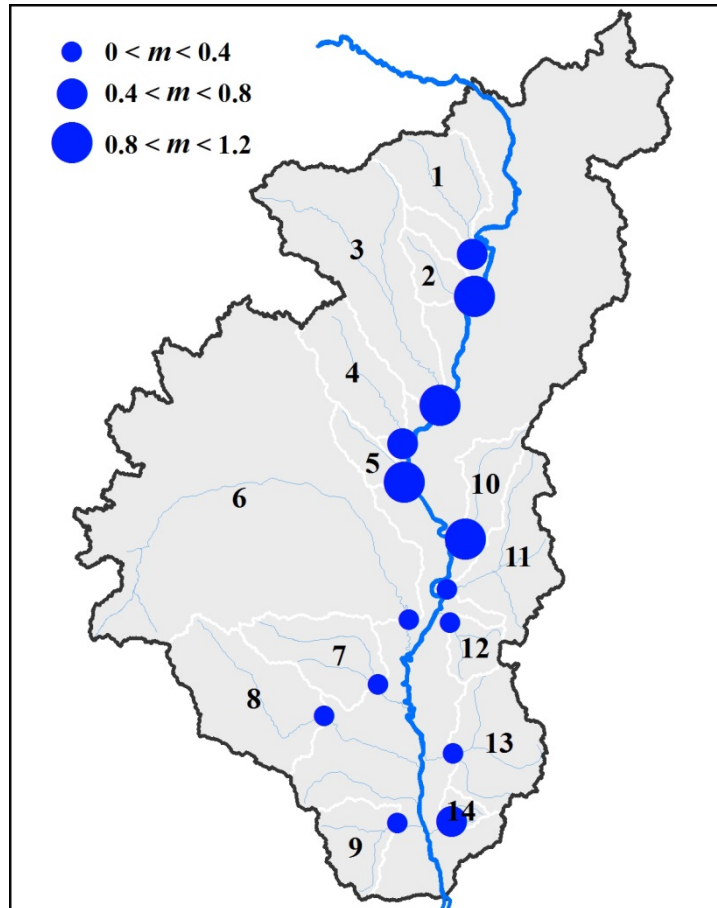


Figure 10. Spatial distribution of slope m in the regression equation $\overline{SC} = -mA_c + n$. \overline{SC} is the decadal average sediment coefficient, and A_c is the percentage of the area affected by soil and water conservation measures in the catchments.

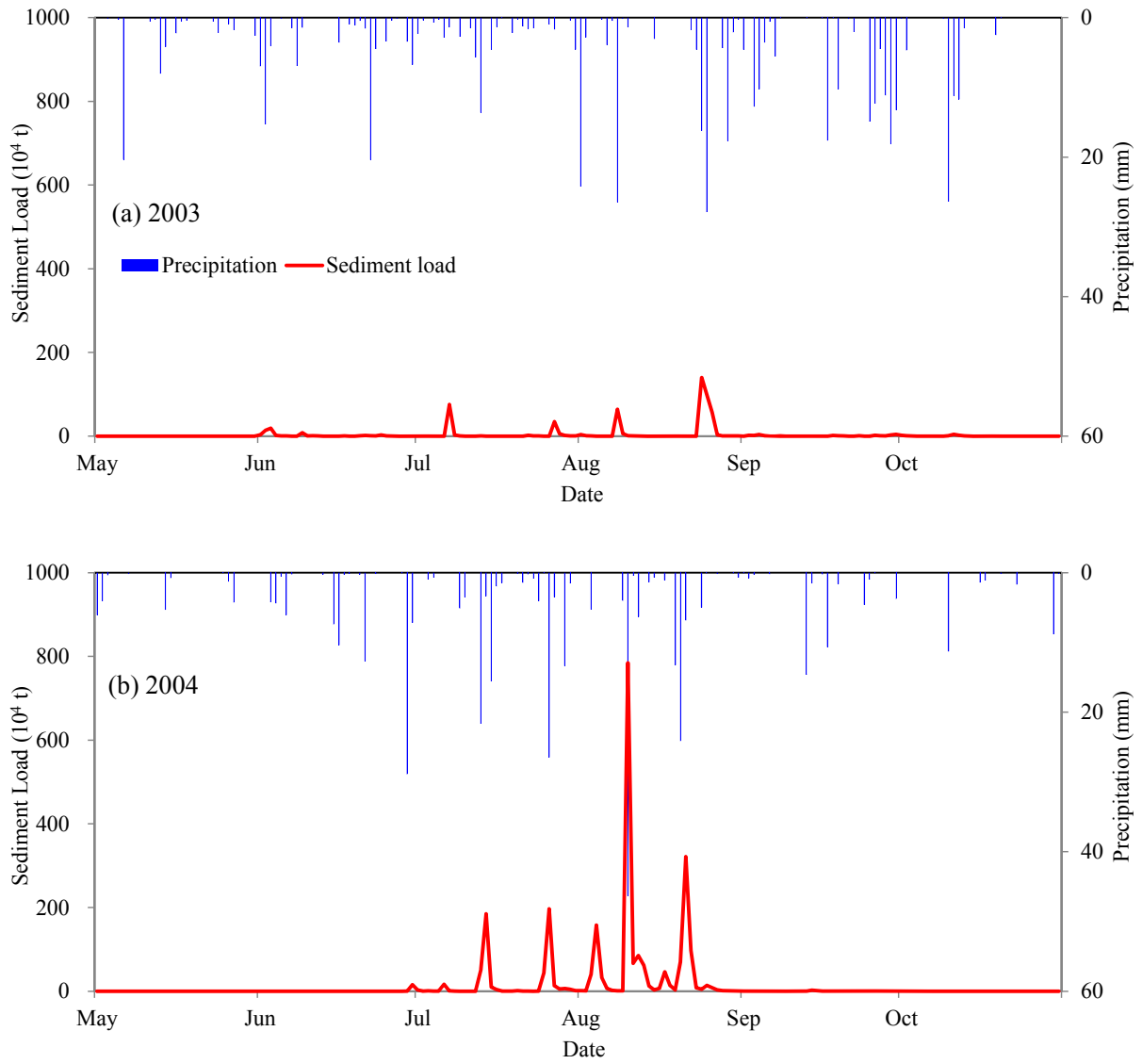


Figure 11. Daily precipitation and sediment load of the Yanhe catchment during rainy season (May-October) in (a) 2003 and (b) 2004.